PHYSICAL REVIEW B **85**, 224510 (2012)

Coexistence of different electronic phases in the $K_{0.8}Fe_{1.6}Se_2$ superconductor: A bulk-sensitive hard x-ray spectroscopy study

L. Simonelli,[1] N. L. Saini,[2] M. Moretti Sala,[1] Y. Mizuguchi,[3,4] Y. Takano,[3,4] H. Takeya,[3,4] T. Mizokawa,[5] and G. Monaco[1]
[1]*European Synchrotron Radiation Facility, Boîte Postale 220, F-38043 Grenoble Cedex, France*
[2]*Dipartimento di Fisica, Universitá di Roma "La Sapienza," Piazzale le Aldo Moro 2, I-00185 Rome, Italy*
[3]*National Institute for Materials Science, 1-2-1 Sengen, Tsukuba 305-0047, Japan*
[4]*JST-TRIP, 1-2-1 Sengen, Tsukuba 305-0047, Japan*
[5]*Department of Physics and Department of Complexity Science and Engineering, University of Tokyo,*
5-1-5 Kashiwanoha, Kashiwa, Chiba 277-8561, Japan

(Received 24 February 2012; revised manuscript received 23 May 2012; published 7 June 2012)

We have studied electronic and magnetic properties of the $K_{0.8}Fe_{1.6}Se_2$ superconductor by x-ray absorption and emission spectroscopy. Detailed temperature-dependent measurements along with a direct comparison with the binary FeSe system have revealed coexisting electronic phases: a majority phase with a high-spin $^{3+}$Fe state and a minority phase with an intermediate-spin $^{2+}$Fe state. The effect of high-temperature annealing suggests that the compressed phase with a lower-spin $^{2+}$Fe state is directly related to the high-T_c superconductivity in the title system. The results clearly underline the glassy nature of superconductivity in the electronically inhomogeneous $K_{0.8}Fe_{1.6}Se_2$, similar to the superconductivity in granular phases.

DOI: 10.1103/PhysRevB.85.224510 PACS number(s): 74.70.Xa, 74.25.Jb, 74.81.Bd

I. INTRODUCTION

The discovery of superconductivity in binary FeSe (11-type) chalcogenide has been an important finding to progress in the understanding of iron-based superconductors.[1] The 11-type chalcogenides have been regarded as model systems to explore the fundamental electronic structure of the iron-based superconductors since, unlike the more common RFeAsO ($R =$ La, Nd, Pr, Sm, Gd) and (Ba, Sr)Fe_2As_2 pnictides, they lack the spacer layers, and hence the central role played by the Fe-Fe plane with interacting anions (pnictogen/chalcogen) can be distinctly identified.

Very recently, FeSe layers have been successfully intercalated by alkaline atoms, with an intercalated $A_xFe_{2-y}Se_2$ (A = K, Rb, Cs) system showing superconductivity up to 32 K,[2–6] unlike the binary FeSe with a maximum $T_c \sim 8$ K. This new $A_xFe_{2-y}Se_2$ (122)-type superconductor displays a large magnetic moment per Fe site, intrinsic Fe vacancy order in the *ab* plane, and an antiferromagnetic order in the *c* direction.[7,8] Several experiments have indicated that the superconductivity occurs only in Fe-deficient samples[9–12] and the ordering of Fe vacancies, important for their electronic and magnetic properties, can be controlled by heat treatments.[8,10,11,13–15] In addition, the system is structurally phase separated at the nanoscale containing an iron-vacancy-ordered phase with an expanded in-plane lattice and a coexisting minority phase with a compressed in-plane lattice.[13] Considering the complexity of the system, it is of vital importance to investigate the coexisting phases for their electronic and magnetic properties.

In this work, we have exploited bulk-sensitive high-energy spectroscopies to probe the coexisting electronic phases in the $K_{0.8}Fe_{1.6}Se_2$ superconductor. We have used x-ray emission (XES) and high-resolution x-ray absorption (XAS) spectroscopy to study the electronic and magnetic properties as a function of thermal cycling. Starting from room temperature (RT), where the system shows a nanoscale phase separation,[13] we cooled the sample across the superconducting transition, and the temperature evolution of the electronic and magnetic properties is monitored while warming up to RT. Later, we annealed the sample up to 606 K and quenched it down to 10 K for a direct comparison between as-grown and annealed samples. The results are discussed along with the electronic and magnetic properties of binary FeSe[16] to distinctly identify the effect of K intercalation on the electronic properties of these superconductors.

II. EXPERIMENTAL DETAILS

Measurements of XES and high-resolution XAS were carried out on a well-characterized as-grown single crystal of $K_{0.8}Fe_{1.6}Se_2$.[3] The experiments were performed at the beam line ID16 of the European Synchrotron Radiation Facility. The experimental setup consists of a spectrometer based on the simultaneous use of a bent analyzer Ge(620) crystal (bending radius $R = 1$ m) and a pixelated position-sensitive Timepix detector[17] in Rowland circle geometry. The scattering plane was horizontal and parallel to the linear polarization vector of the incident x-rays beam. The measurements were carried out fixing the sample surface (the *ab* plane of the $K_{0.8}Fe_{1.6}Se_2$ single crystal) at $\sim 45^\circ$ from the incoming beam direction and the scattering angle 2θ at $\sim 90^\circ$. The total energy resolution was about 1.1 eV full width at half maximum. The samples were placed in a cryogenic environment, and the temperature was controlled with an accuracy of ± 1 K.

III. RESULTS AND DISCUSSIONS

Figure 1(a) shows normalized Fe K-edge partial fluorescence yield (PFY) absorption spectra of $K_{0.8}Fe_{1.6}Se_2$, collected at different temperatures, obtained by collecting the Fe $K\beta_{1,3}$ emission intensity and scanning the incident energy across the absorption edge. The spectra are normalized with respect to the atomic absorption estimated by a linear fit far away from the absorption edge. The K-edge absorption process is mainly governed by the $1s \rightarrow \epsilon p$ dipole transition. In addition, the

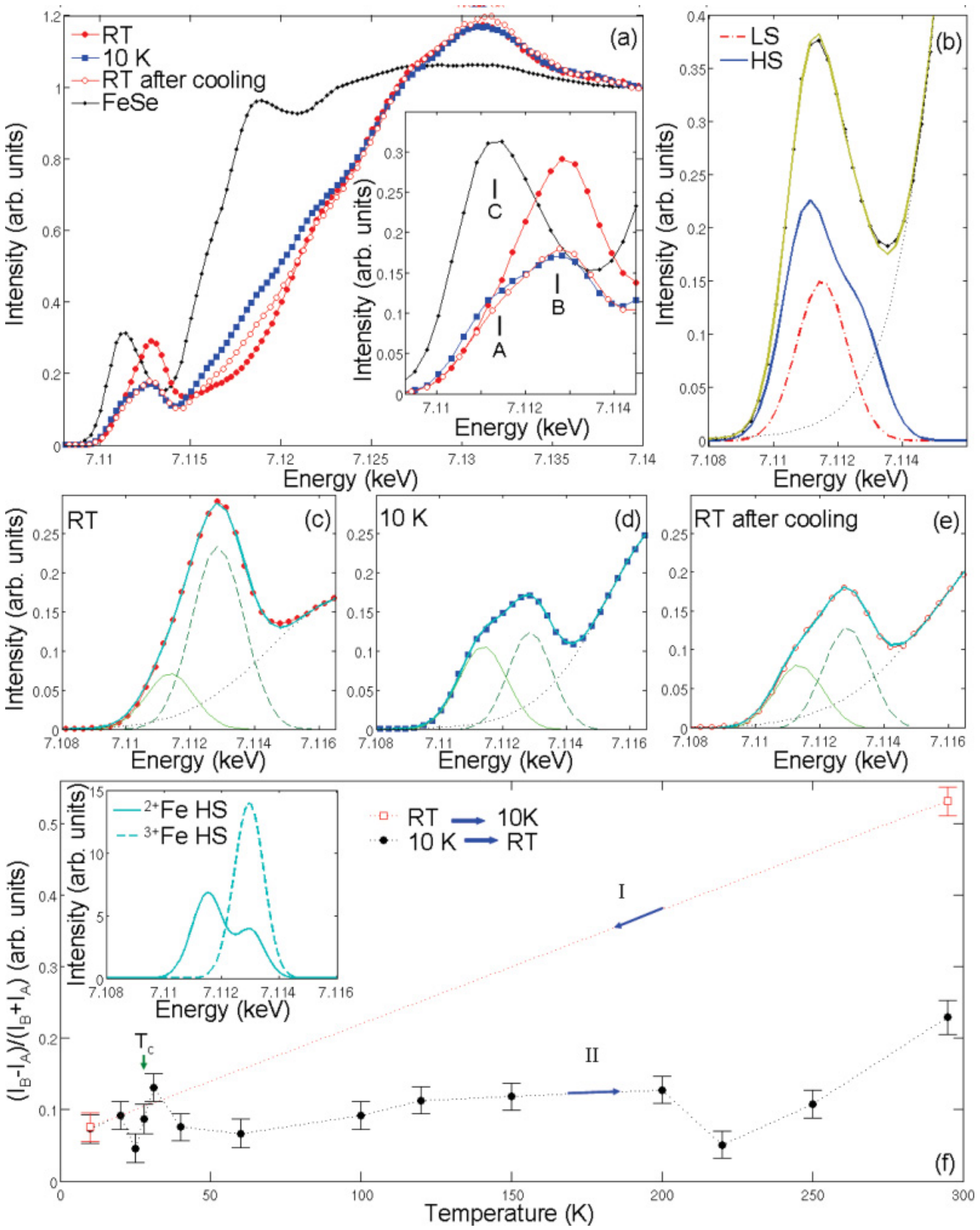

FIG. 1. (Color online) (a) PFY spectra measured at the Fe K edge of $K_{0.8}Fe_{1.6}Se_2$ at RT, 10 K, and RT after cooling, compared with the PFY spectrum of binary FeSe. The inset shows a close-up of the prepeak region. (b) The prepeak of FeSe is shown deconvoluted in two components representing the low (dot-dashed line) and high (solid line) spin $^{2+}$Fe states. (c)–(e) The prepeak of $K_{0.8}Fe_{1.6}Se_2$ is deconvoluted in two Gaussian features, A and B. (f) Temperature cycle of the relative intensities of the two features, $(I_B - I_A)/(I_B + I_A)$, while cooling down (I) followed by warming up to RT again (II). The inset represents theoretical simulation of the preedge region for tetrahedral high-spin $^{2+}$Fe (solid line) and $^{3+}$Fe (dashed line) complexes.[19]

spectra show strong prepeak features due to direct $1s \rightarrow 3d$ quadrupole transitions to the unoccupied Fe *3d* hybridized with Se *4p* states.[18] In the crystal-field picture the prepeak is sensitive to the electronic structure, and its energy position, splitting, and intensity distribution change systematically with spin state, oxidation state, and local geometry.[19] The differences between FeSe and $K_{0.8}Fe_{1.6}Se_2$ are evident. FeSe exhibits a broad and asymmetric single prepeak feature C at $E_C \approx 7111.1$ eV (typical of $^{2+}$Fe complexes[20]), unlike $K_{0.8}Fe_{1.6}Se_2$, for which the prepeak is composed by a doublet feature [see, e.g., the inset of Fig. 1(a) showing a close-up of the prepeak]. The large width and asymmetry of the FeSe prepeak feature indicate that this system may not be a simple low-spin $^{2+}$Fe complex; rather, it should contain both low-spin (LS) and high-spin (HS) $^{2+}$Fe states. Indeed, as shown in Fig. 1(b), the FeSe prepeak can be deconvoluted in two components due to LS and HS $^{2+}$Fe states.[19] FeSe shows then an intermediate-spin $^{2+}$Fe state, consistent with the local Fe moment of about $2\ \mu_B$.[21] On the other hand, the PFY spectra of $K_{0.8}Fe_{1.6}Se_2$ apparently show a prepeak with two features, A and B, appearing at $E_A \approx 7111.4$ and $E_B \approx 7112.9$ eV. Since the system displays a large local Fe moment of about 3.3 μ_B,[8,21,22] we expect a doubled absorption prepeak to mainly represent the HS $^{2+}$Fe state (however, with the a more intense feature at lower energy than expected theoretically[19]). The fact that the spectral weight is higher at the higher energy means that the HS $^{3+}$Fe state should coexist with the HS $^{2+}$Fe state [see, e.g., inset of Fig. 1(f), which shows calculated prepeaks for tetrahedral HS $^{2+}$Fe and $^{3+}$Fe complexes]. This constructs direct evidence of coexisting electronic phases with different spin states in the $K_{0.8}Fe_{1.6}Se_2$ system.

Several experiments have revealed an intrinsic phase separation in the $K_{0.8}Fe_{1.6}Se_2$ system[23–25] below ∼580 K, where the iron-vacancy-ordered structure is associated with the magnetic order.[8,26,27] Along with the majority phase, a minority phase with a slightly compressed in-plane lattice appears.[23] It is likely that the two phases have different electronic properties due to local change of the Fe valence in different sublattices due to the high K mobility and distribution. In fact, the PFY spectra provide clear evidence of electronic phase separation, consistent with the structural nematicity of the system. The in-plane compressed (out-of-plane expanded) minority phase most likely corresponds to a $^{2+}$Fe oxidation state, while the in-plane expanded (out-of-plane compressed) phase corresponds to vacancy ordering to a $^{3+}$Fe state. Despite the fact that the phase separation affects both in-plane and out-of-plane axes, the variation of the c axis is 50% larger than that along the a,b directions. Consistently, the shift of the absorption edge reflects the fact that a c-axis expanded (compressed) phase corresponds to a lower (higher) energy.

In order to investigate the temperature evolution of the electronic phase separation, we have deconvoluted the prepeak of $K_{0.8}Fe_{1.6}Se_2$ in two Gaussian features, A and B, with fixed energy positions [Figs. 1(c)–1(e)]. A pseudo-Voigt function was used to describe the background due to the rising edge (dotted curve). The width of A has been kept fixed, while that of B was variable to compensate for the effect of the background subtraction. Figure 1(f) displays relative intensity, $(I_B - I_A)/(I_B + I_A)$, representing the qualitative evolution of the coexisting electronic phases. Starting from RT and cooling down to 10 K, B loses and A gains intensity. This may be due to a reorganization between nanoscale phases while the sample is cooled. Warming up again to RT, different from B, feature A approximately recovers its initial intensity; however, the distribution of the phases appears to be different. The temperature dependence of the relative intensity also reveals a small discontinuity across T_c. Moreover, a domelike anomaly is evident between 100 and 220 K, similar to the resistivity anomaly seen in this system.[12,14,28,29] It should be noted that the Fe-Se bond length does not show any change with temperature.[30,31] This implies negligible change in the Fe-Se $3d$-$4p$ hybridization.[18] Therefore the absorption prepeak, consisting of HS $^{2+}$Fe and HS $^{3+}$Fe components, gets redistributed without any appreciable effect of structural changes with temperature.

Independent and complementary information on the electronic and magnetic properties of the Fe $3d$ levels can be obtained from XES. Figure 2(a) shows the Fe Kβ emission line measured on $K_{0.8}Fe_{1.6}Se_2$ at different temperatures along with the RT XES spectra of FeSe and SmFeAsO systems. In the crystal-field picture the overall spectral shape is dominated by the $(3p,3d)$ exchange interactions.[32] In particular, the presence (absence) of a pronounced feature at lower energy (Kβ') is an indication of a HS (LS) state of Fe.[32] Also, the energy position of the K$\beta_{1,3}$ provides information on the spin state reflecting the effective number of unpaired $3d$

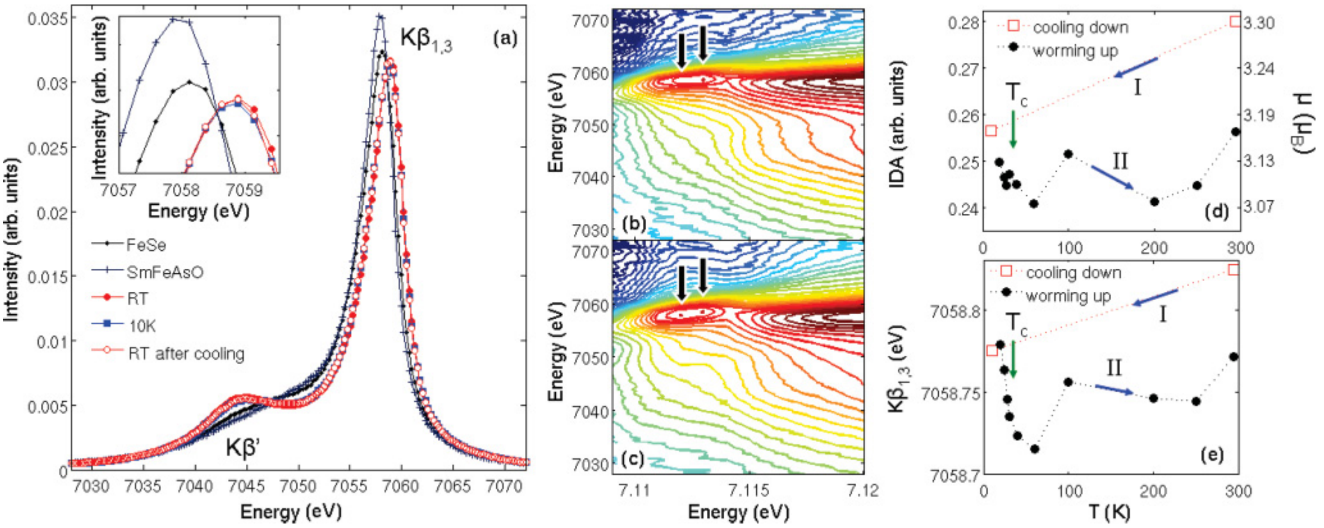

FIG. 2. (Color online) (a) Fe Kβ emission spectra of $K_{0.8}Fe_{1.6}Se_2$ at different temperatures, compared with the spectra measured on FeSe and SmFeAsO. The spectra are normalized to the integrated area. The inset shows a close-up of the main K$\beta_{1,3}$ emission line. (b) and (c) Resonant x-ray emission maps at RT and 10 K, respectively, measured at the Kβ emission line with the incoming energy around the absorption prepeak. The arrows indicate the two features resonating at E_A and E_B. (d) IDA as a function of temperature. Open squares represent the data while cooling down the sample (I), and the solid circles represent warming up from 10 K (II). The scale on the right-hand side shows the local magnetic moment μ determined following Gretarsson *et al.*[21] (e) Energy position of the K$\beta_{1,3}$ main line as a function of temperature. The uncertainties are of the order of the symbols size.

electrons.[32] Differences between the XES of $K_{0.8}Fe_{1.6}Se_2$, FeSe, and SmFeAsO are evident.

In Figs. 2(b) and 2(c) we have displayed the resonant x-ray emission maps collected at the Fe Kβ emission with the incoming energy around the absorption prepeak. The RT map in Fig. 2(b) shows a main feature and a shoulder, resonating at E_B and E_A, respectively. The map measured at 10 K instead [Fig. 2(c)] reveals a clear enhancement of the shoulder intensity, appearing as a distinct feature at a lower emitted energy. This is a clear indication that the prepeak feature A should be related to a lower-spin state than feature B, in agreement with the hypothesis that features A and B correspond to the HS $^{2+}$Fe and $^{3+}$Fe phases, respectively. Therefore, the minority phase has a reduced local Fe moment with respect to the Fe-vacancy-ordered phase. The observation further underlines the correlation between the Fe vacancy order and local Fe moment in the title system.

It is possible to quantify the local Fe moment from the integrated area of absolute XES difference with respect to a LS reference.[21] Since SmFeAsO is almost nonmagnetic,[21] we have taken SmFeAsO as a reference to obtain the integrated absolute difference (IDA), which is approximately proportional to the spin magnetic moment. In order to determine the relative variation in the magnetic moment, we have used the RT value of μ for $K_{0.8}Fe_{1.6}Se_2$ [3.3 μ_B (Refs. 8,21,22)] and for FeSe [2μ_B (Ref. 21)]. Figures 2(d) and 2(e) show the temperature dependence of the IDA and the energy position of the K$\beta_{1,3}$ main line. Since the two quantities provide the same information, qualitatively similar trends are observed. The changes in the Kβ emission are very much consistent with those appearing in the absorption prepeak, showing a reduced magnetic moment at low temperature due to the redistribution of the phases characterized by the HS $^{2+}$Fe and HS $^{3+}$Fe states. More quantitatively, cooling down, we observe a reduction of the local Fe moment from 3.30 to 3.17 μ_B. Comparing the corresponding change in the PFY spectra, the reduction of the Fe moment is too small if we consider the minority phase being in low-spin $^{2+}$Fe with no local moment, confirming the dominance of the high-spin $^{2+}$Fe state. In the temperature range from 10 to 60 K, μ continues to

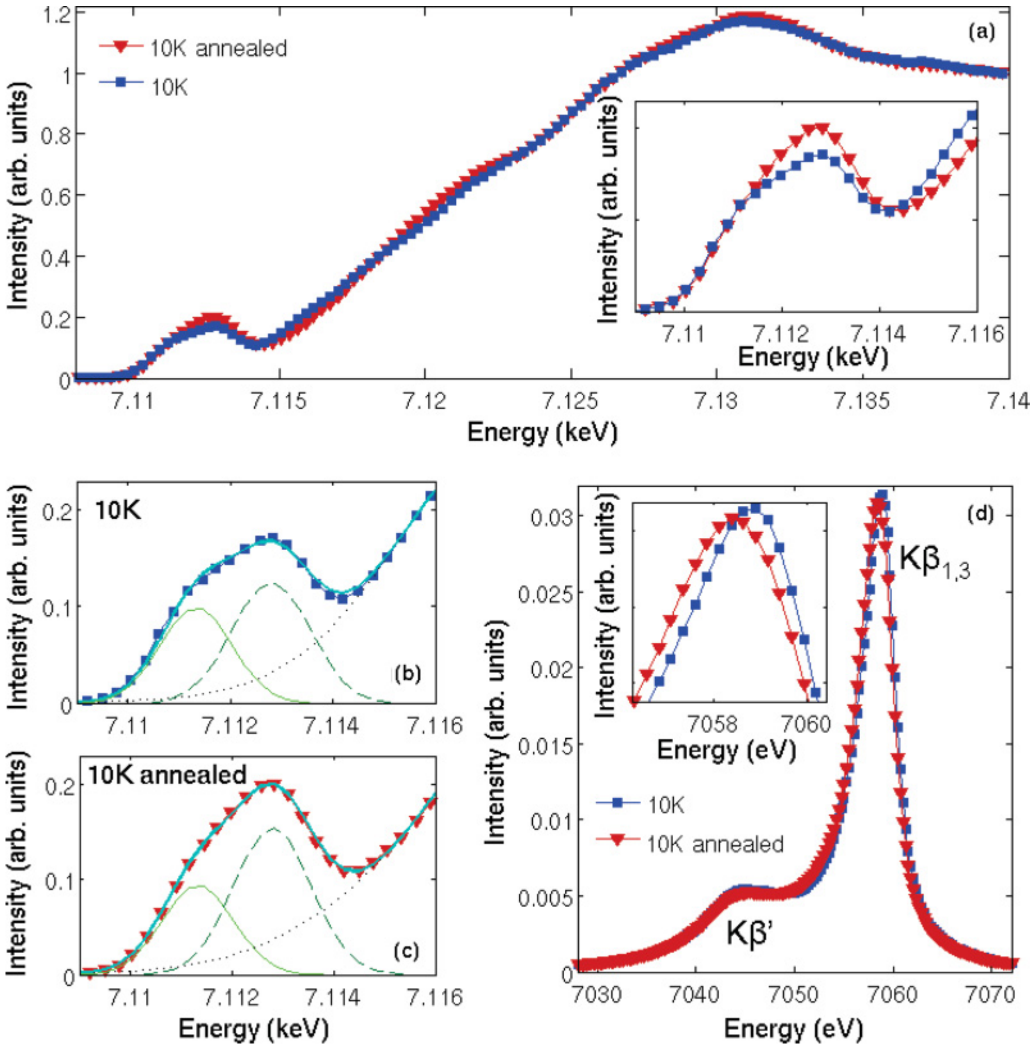

FIG. 3. (Color online) (a) PFY spectrum at the Fe K edge of $K_{0.8}Fe_{1.6}Se_2$ measured at 10 K after high-temperature annealing (triangles), compared with the PFY spectrum on the as-grown sample (squares). The inset shows a close-up of the prepeak region. (b) and (c) The prepeaks before and after annealing are shown deconvoluted in two Gaussian components. (d) Comparison of the Fe Kβ emission spectra collected at 10 K on the sample as-grown (squares) and after the high-temperature annealing (triangles).

decrease down to a minimum of 3.08 μ_B, unlike the negligible change seen in the PFY. With a further increase in temperature, the local Fe moment μ appears to show a dome-shaped anomalous variation around 150 K, which might be related to the resistivity anomaly.[12,14,28,29] This kind of anomalous behavior can be expected from an inhomogeneous and glassy system with coexisting phases.

The glassy nature of $K_{0.8}Fe_{1.6}Se_2$ is also evident from the effect of thermal cycling. To get further insight we have annealed the sample at 606 K for 20 min and quenched it down to 10 K. Figure 3(a) shows the PFY spectrum after this treatment, compared with the earlier one at 10 K. There is an apparent change in the prepeak, with component B showing a relative increase after the annealing [Figs. 3(b) and 3(c)]. On the other hand, the Kβ emission spectra reveal a clear decrease in the Fe moment [Fig. 3(d)]. Indeed, the IDA for the annealed sample is ∼0.187, which corresponds to $\mu \sim 2.79\ \mu_B$ (to be compared with $\mu \sim 3.17\ \mu_B$ for the as-grown sample), which is more similar to the moment for the binary FeSe.[21] Therefore, the XES results are consistent with an increase of the lower-spin $^{2+}$Fe state by annealing. Apparently this is inconsistent with the PFY spectra in which feature B has been assigned to the high-spin $^{3+}$Fe state. However, we should recall that the PFY of FeSe goes through a large change, with the prepeak shifting towards higher energy under hydrostatic pressure[33] while the superconducting transition temperature changes from a low (8 K) to a high (37 K) value. Thus an intensity increase of feature B in the PFY seems to be due to a compressed low-spin $^{2+}$Fe phase. Therefore, a distribution of different phases is likely, with even lower magnetic moment (most likely related to compressed FeSe filaments in the texture of the magnetic phase), which could be involved in the high-T_c superconductivity of the $K_{0.8}Fe_{1.6}Se_2$ system. Indeed, the system is characterized by a large disorder and a glassy local structure,[30] similar to granular materials.

IV. CONCLUSIONS

In conclusion, we have investigated the evolution of the electronic and magnetic properties of $K_{0.8}Fe_{1.6}Se_2$ by XAS and XES measurements as a function of temperature in a close thermal cycle, providing clear evidence of coexisting electronic phases characterized by different Fe valences and local magnetic moments. Using resonant XES, we have found that the Fe-vacancy-ordered (disordered compressed) phase corresponds to HS $^{3+}$Fe (intermediate-spin $^{2+}$Fe). The presence of the HS $^{3+}$Fe phase means that the minority superconducting phase is heavily electron doped, consistent with the absence of the hole pockets on the Fermi surface.[34,35] We also find that the local Fe moment sustains a substantial reduction under high-temperature annealing due to disordering of the Fe vacancies. A comparative study with respect to FeSe suggests that high T_c in the title system has a clear analogy with the increased T_c of binary FeSe under hydrostatic pressure. It looks like the coexistence of different phases is the key, and since by annealing the disorder increases with a simultaneous decrease of the local Fe moment, it is likely that a fraction of a different metallic compressed disordered phase in a lower-spin configuration[25] exists. These filamentary phases become superconducting, which also happens in granular superconductors.

---

[1] Y. Mizuguchi and Y. Takano, J. Phys. Soc. Jpn. **79**, 102001 (2010).

[2] J. Guo, S. Jin, G. Wang, S. Wang, K. Zhu, T. Zhou, M. He, and X. Chen, Phys. Rev. B **82**, 180520 (2010).

[3] Y. Mizuguchi, H. Takeya, Y. Kawasaki, T. Ozaki, S. Tsuda, T. Yamaguchi, and Y. Takano, Appl. Phys. Lett. **98**, 042511 (2011).

[4] J. J. Ying, X. F. Wang, X. G. Luo, A. F. Wang, M. Zhang, Y. J. Yan, Z. J. Xiang, R. H. Liu, P. Cheng, G. J. Ye, and X. H. Chen, Phys. Rev. B **83**, 212502 (2011).

[5] A. Krzton-Maziopa, Z. Shermadini, E. Pomjakushina, V. Pomjakushin, M. Bendele, A. Amato, R. Khasanov, H. Luetkens, and K. Conder, J. Phys. Condens. Matter **23**, 052203 (2011).

[6] M. Fang, H. Wang, C. Dong, Z. Li, C. Feng, J. Chen, and H. Q. Yuan, Europhys. Lett. **94**, 27009 (2011).

[7] D. H. Ryan, W. N. Rowan-Weetaluktuk, J. M. Cadogan, R. Hu, W. E. Straszheim, S. L. Bud'ko, and P. C. Canfield, Phys. Rev. B **83**, 104526 (2011).

[8] Bao Wei, Huang Qing-Zhen, Chen Gen-Fu, M. A. Green, Wang Du-Ming, He Jun-Bao, and Qiu Yi-Ming, Chin. Phys. Lett. **28**, 086104 (2011).

[9] J. Guo, X. Chen, C. Zhang, J. Guo, X. Chen, Q. Wu, D. Gu, P. Gao, X. Dai, L. Yang, H. Mao, L. Sun, Z. Zhao, Phys. Rev. Lett. **108**, 197001 (2012); Y. Kawasaki, Y. Mizuguchi, K. Deguchi, T. Watanabe, T. Ozaki, S. Tsuda, T. Yamaguchi, Hiroyuki Takeya, Y. Takano, arXiv:1101.0896; J. J. Ying, X. F. Wang, X. G. Luo, Z. Y. Li, Y. J. Yan, M. Zhang, A. F. Wang, P. Cheng, G. J. Ye, Z. J. Xiang, R. H. Liu, and X. H. Chen, New J. Phys. **13**, 033008 (2011).

[10] D. M. Wang, J. B. He, T.-L. Xia, and G. F. Chen, Phys. Rev. B **83**, 132502 (2011).

[11] A. M. Zhang, J. H. Xiao, J. B. He, D. M. Wang, G. F. Chen, and Q. M. Zhang, Phys. Rev. B **85**, 024518 (2012).

[12] Y. J. Yan, M. Zhang, A. F. Wang, J. J. Ying, Z. Y. Li, W. Qin, X. G. Luo, J. Q. Li, J. Hu, and X. H. Chen, Sci. Rep. **2**, 212 (2012).

[13] A. Ricci, N. Poccia, B. Joseph, G. Arrighetti, L. Barba, J. Plaisier, G. Campi, Y. Mizuguchi, H. Takeya, Y. Takano, N. L. Saini, and A. Bianconi, Supercond. Sci. Technol. **24**, 082002 (2011).

[14] F. Han, B. Shen, Z.-Y. Wang, and H.-H. Wen, arXiv:1103.1347.

[15] V. Svitlyk, D. Chernyshov, E. Pomjakushina, A. Krzton-Maziopa, K. Conder, V. Pomjakushin, and V. Dmitriev, Inorg. Chem. **50**, 10703 (2011).

[16] L. Simonelli, N. L. Saini, Y. Mizuguchi, Y. Takano, T. Mizokawa, G. Baldi, and G. Monaco (unpublished).

[17] C. Ponchut, J. M. Rigal, J. Clément, E. Papillon, A. Homs, and S. Petitdemange, J. Instrum. **6**, C01069 (2011).

[18] B. Joseph, A. Iadecola, L. Simonelli, Y. Mizuguchi, Y. Takano, T. Mizokawa, and N. L. Saini, J. Phys. Condens. Matter **22**, 485702 (2010).

[19] T. E. Westre, P. Kennepohl, J. G. DeWitt, B. Hedman, K. O. Hodgson, and E. I. Solomon, J. Am. Chem. Soc. **119**, 6297 (1997).

[20] B. C. Chang, Y. B. You, T. J. Shiu, M. F. Tai, and H. C. Ku, Y. Y. Hsu, L. Y. Jang, J. F. Lee, Z. Wei, K. Q. Ruan, and X. G. Li, Phys. Rev. B **80**, 165108 (2009); A. Ignatov, C. L. Zhang, M. Vannucci, M. Croft, T. A. Tyson, D. Kwok, Z. Qin, and S.-W. Cheong, arXiv:0808.2134.

[21] H. Gretarsson, A. Lupascu, J. Kim, D. Casa, T. Gog, W. Wu, S. R. Julian, Z. J. Xu, J. S. Wen, G. D. Gu, R. H. Yuan, Z. G. Chen, N.-L. Wang, S. Khim, K. H. Kim, M. Ishikado, I. Jarrige, S. Shamoto, J.-H. Chu, I. R. Fisher, and Y.-J. Kim, Phys. Rev. B **84**, 100509(R) (2011).

[22] X.-W. Yan, M. Gao, Z.-Y. Lu, and T. Xiang, Phys. Rev. B **83**, 233205 (2011).

[23] A. Ricci, N. Poccia, G. Campi, B. Joseph, G. Arrighetti, L. Barba, M. Reynolds, M. Burghammer, H. Takeya, Y. Mizuguchi, Y. Takano, M. Colapietro, N. L. Saini, and A. Bianconi, Phys. Rev. B **84**, 060511(R) (2011).

[24] Z. Wang, Y. J. Song, H. L. Shi, Z. W. Wang, Z. Chen, H. F. Tian, G. F. Chen, J. G. Guo, H. X. Yang, and J. Q. Li, Phys. Rev B **83**, 140505(R) (2011).

[25] F. Chen, M. Xu, Q. Q. Ge, Y. Zhang, Z. R. Ye, L. X. Yang, J. Jiang, B. P. Xie, R. C. Che, M. Zhang, A. F. Wang, X. H. Chen, D. W. Shen, X. M. Xie, M. H. Jiang, J. P. Hu, and D. L. Feng, Phys. Rev. X **1**, 021020 (2011).

[26] Z. Shermadini, A. Krzton-Maziopa, M. Bendele, R. Khasanov, H. Luetkens, K. Conder, E. Pomjakushina, S. Weyeneth, V. Pomjakushin, O. Bossen, and A. Amato, Phys. Rev. Lett. **106**, 117602 (2011); V. Yu. Pomjakushin, D. V. Sheptyakov, E. V. Pomjakushina, A. Krzton-Maziopa, K. Conder, D. Chernyshov, V. Svitlyk, and Z. Shermadini, Phys. Rev. B **83**, 144410 (2011).

[27] R. H. Liu, X. G. Luo, M. Zhang, A. F. Wang, J. J. Ying, X. F. Wang, Y. J. Yan, Z. J. Xiang, P. Cheng, G. J. Ye, Z. Y. Li, and X. H. Chen, Europhys. Lett. **94**, 27008 (2011).

[28] W. Bao, G. N. Li, Q. Huang, G. F. Chen, J. B. He, M. A. Green, Y. Qiu, D. M. Wang, and J. L. Luo, arXiv:1102.3674v1.

[29] M.-H. Fang, H.-D. Wang, C.-H. Dong, Z.-J. Li, C.-M. Feng, J. Chen, and H. Q. Yuan, Europhys. Lett. **94**, 27009 (2011).

[30] A. Iadecola, B. Joseph, L. Simonelli, A. Puri, Y. Mizuguchi, H. Takeya, Y. Takano, and N. L. Saini, J. Phys. Condens. Matter **24**, 115701 (2012).

[31] T. A. Tyson, T. Yu, S. J. Han, M. Croft, G. D. Gu, I. K. Dimitrov, and Q. Li, Phys. Rev. B **85**, 024504 (2012).

[32] P. Glatzel and U. Bergmann, Coord. Chem. Rev. **249**, 65 (2005).

[33] J. M. Chen, S. C. Haw, J. M. Lee, T. L. Chou, S. A. Chen, K. T. Lu, Y. C. Liang, Y. C. Lee, N. Hiraoka, H. Ishii, K. D. Tsuei, E. Huang, and T. J. Yang, Phys. Rev. B **84**, 125117 (2011).

[34] L. Zhao, D. Mou, S. Liu, X. Jia, J. He, Y. Peng, L. Yu, X. Liu, G. Liu, S. He, X. Dong, J. Zhang, J. B. He, D. M. Wang, G. F. Chen, J. G. Guo, X. L. Chen, X. Wang, Q. Peng, Z. Wang, S. Zhang, F. Yang, Z. Xu, C. Chen, and X. J. Zhou, Phys. Rev. B **83**, 140508 (2011).

[35] T. Qian, X.-P. Wang, W.-C. Jin, P. Zhang, P. Richard, G. Xu, X. Dai, Z. Fang, J.-G. Guo, X.-L. Chen, and H. Ding, Phys. Rev. Lett. **106**, 187001 (2011).